cosmetics

MDPI

Article

Molecular Docking Simulation of Phenolics towards Tyrosinase, Phenolic Content, and Radical Scavenging Activity of Some Zingiberaceae Plant Extracts

Mutakin [1,*], Nyi Mekar Saptarini [1], Riezki Amalia [2], Sri Adi Sumiwi [2], Sandra Megantara [1], Febrina Amelia Saputri [3] and Jutti Levita [2,*]

[1] Department of Pharmaceutical Analysis and Medicinal Chemistry, Faculty of Pharmacy, Padjadjaran University, Sumedang 45363, Indonesia; nyi.mekar@unpad.ac.id (N.M.S.); s.megantara@unpad.ac.id (S.M.)
[2] Department of Pharmacology and Clinical Pharmacy, Faculty of Pharmacy, Padjadjaran University, Sumedang 45363, Indonesia; riezki.amalia@unpad.ac.id (R.A.); sri.adi@unpad.ac.id (S.A.S.)
[3] Faculty of Pharmacy, Universitas Indonesia, Depok 16424, Indonesia; febrina.amelia@farmasi.ui.ac.id
* Correspondence: mutakin@unpad.ac.id (M.); jutti.levita@unpad.ac.id (J.L.)

Abstract: In Indonesia, plants have been indigenously used to treat various diseases and as cosmetics. It is always challenging to explore the molecular interactions of phenolic compounds towards the levels of constituents that contribute to the biological activities of plants. This study aimed to select a plant of the Zingiberaceae family with the highest phenolics and flavonoids, the strongest radical scavenging activity, and the best interaction towards tyrosinase in terms of docking score and binding mode. Initially, the total phenolics and radical scavenging capacity of Zingiberaceae plants, namely, *Hedychium coronarium*, *Curcuma zedoaria*, *Curcuma heyneana*, and *Alpinia galanga*, were determined using the Folin–Ciocâlteu method and the 1,1-diphenyl-2-picrylhydrazyl (DPPH) assay. The main phytoconstituents of plants with the highest phenolic levels were docked to the binding site of tyrosinase. Three anti-melanogenesis agents commonly used in cosmetics, namely, arbutin, hydroquinone, and kojic acid, were used as the standard. Our study revealed that all the tested plants contain polyphenolic compounds in the range of 17.92 (*C. zedoaria* rhizome extract) to 252.36 (*A. galanga* rhizome extract) mg GAE/g and have radical scavenging capacity, with IC_{50} values in the range of 66.67 (*A. galanga* rhizome extract) to 320.0 (*C. heyneana* rhizome extract) µg/mL. A molecular docking simulation demonstrated that four constituents, i.e., kaempferol, galangin, ethyl *p*-methoxycinnamate, and 6-gingerol, could occupy the binding site of tyrosinase with prominent affinity and interact with essential residues of the enzyme. This study confirms that *Alpinia galanga* possesses the potential to be further developed as a cosmetic with a radical scavenging and tyrosinase inhibitory activity. However, it may be interesting to carry out further studies of how the plant extract affects the melanogenesis signaling pathway.

Keywords: *Alpinia galanga*; anti-melanogenesis; antioxidant; flavonols; galangin; quercetin

Citation: Mutakin; Saptarini, N.M.; Amalia, R.; Sumiwi, S.A.; Megantara, S.; Saputri, F.A.; Levita, J. Molecular Docking Simulation of Phenolics towards Tyrosinase, Phenolic Content, and Radical Scavenging Activity of Some Zingiberaceae Plant Extracts. *Cosmetics* **2023**, *10*, 149. https://doi.org/10.3390/cosmetics10060149

Academic Editor: Antonio Vassallo

Received: 19 August 2023
Revised: 26 September 2023
Accepted: 9 October 2023
Published: 31 October 2023

1. Introduction

Despite the vast advances of modern medications, in Asian and African countries, plants are still utilized as the first choice in reducing symptoms of disease. Tropical plants have been indigenously used to treat various disorders. An analysis of articles indexed in the Scopus database described that plants of the families Asteraceae, Fabaceae, Lamiaceae, and Zingiberaceae had been the focus of interest in many drug discovery studies (14,652 articles). From the years of 2015 to 2019, the most-studied topics of medicinal plants were centered on cancer, antidiabetic, and anti-inflammatory activities [1].

The numerous biological activities of medicinal plants are thought to originate from the secondary metabolite contents, among which are the phenolic compounds that contain

hydroxylated aromatic rings, the hydroxy group being attached directly to the phenyl or substituted phenyl, as well as the flavonols [2]. Flavonols, which rank the highest in the number of the flavonoids class, are subcategorized as 2-benzo-γ-pirone. Quercetin (depicted in Figure 1), contained in almost all plants, is one of the most popular flavonols with its unsaturated double bond C2=C3 that extends pi-conjugation onto the carbonyl group in the C-ring, providing a strong radical scavenging capacity [3]. The ultraviolet spectra of flavonols are characterized by two main peaks; the band I belongs to the cinnamoyl moiety at 320–385 nm (showing the electromagnetic radiation absorption of ring B), and band II belongs to the benzoyl moiety at 250–285 nm ring A (showing the electromagnetic radiation absorption of ring A) [4]. Moreover, a catechol moiety also donates antioxidant activity [5,6].

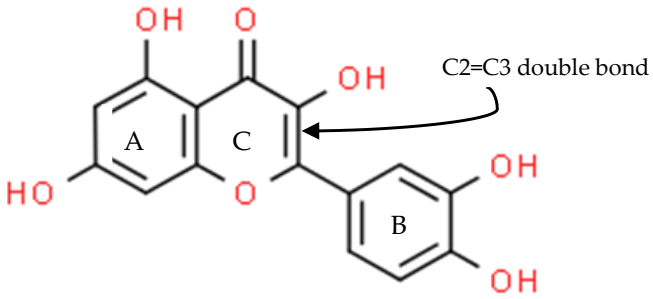

Figure 1. Two-dimensional chemical structure of quercetin (downloaded from http://www.chemspider.com/ with ChemSpider ID 12269344; accessed on 10 August 2023). The C2=C3 double bond is indicated by a curved arrow. Quercetin belongs to the flavonoid class with a general structure of a 15-carbon skeleton, comprised of two phenyl rings (A and B) and a heterocyclic ring (C).

Plants of the families Zingiberaceae, Asteraceae, Acanthaceae, and Fabaceae contain the highest number of medicinal properties, while the most-used parts are the leaves, roots, fruits, rhizomes, whole plants, flowers, seeds, and barks [7]. An in vitro study reported that flavonols from the *Heterotheca inuloides* rhizome, namely, galangin, kaempferol, and quercetin, could inhibit melanogenesis by suppressing tyrosinase activity via chelation with copper in the catalytic site of the enzyme [8]. Moreover, the aqueous acetone extract of *Alpinia officinarum* rhizomes inhibits melanogenesis in theophylline-stimulated murine B164A5 melanoma cells. Two flavonols (kaempferide and galangin) were reported to reduce melanogenesis with IC_{50} values in the range of 10–48 μM [9]. Another flavonol of Zingiberaceae plants, namely, 6-shogaol, had shown suppression toward the activity of tyrosinase, melanin formation, and the expression levels of tyrosinase-related protein 1 (TRP-1) and microphthalmia-associated transcriptional factor (MITF) [10].

Molecular docking studies of polyphenolic compounds have been reported towards human pancreatic alpha-amylase for antidiabetics [11,12]; towards alpha-glucosidase for antidiabetics [12]; towards the main protease enzymes for antivirals [13]; towards β-lactoglobulin for antioxidants [14]; towards all non-redundant holo-proteins from the Protein Data Bank for antioxidative, anti-inflammatory, anticarcinogenic, and antimicrobial activities [15]; and towards cyclooxygenases for anti-inflammatory activities [16]. No studies have been reported on tyrosinase for anti-melanogenesis drug discovery.

Considering this, our study aimed to discover plants with tyrosinase inhibitory activity. This study was started by determining the total phenolics (via the Folin–Ciocalteu method) and the radical scavenging capacity (1,1-diphenyl-2-picrylhydrazyl assay) of plants of the family Zingiberaceae, i.e., *Hedychium coronarium*, *Curcuma zedoaria*, *Curcuma heyneana*, and *Alpinia galanga*. The plant with the highest total phenolic level was further studied for its binding mode toward tyrosinase to predict the potential of the anti-melanogenesis activity.

2. Materials and Methods

2.1. Plant Materials

The plants were collected from Lembang, West Java, Indonesia, and were taxonomically identified by botanists at the Department of Biology, Faculty of Mathematics and Natural Sciences, Universitas Padjadjaran, Indonesia. The samples were confirmed as *Hedychium coronarium* (no. 450/HB/2017), *Curcuma zedoaria* (*Zingiberaceae*) (no. 3742/PL/2019), *Curcuma heyneana* (Zingiberaceae) (no. 3744/PL/2019), and *Alpinia galanga* (Zingiberaceae) (no. 3748/PL/2019).

2.2. Chemicals

The chemicals for the phytochemical screening were freshly prepared, e.g., the Dragendorff reagent (a mixture of basic bismuth nitrate, tartaric acid, and potassium iodide in distilled water) [17], the Lieberman–Burchard reagent (a mixture of concentrated sulfuric acid and acetic anhydride) [18], a lead acetate solution, hydrochloric acid 1N, an ammonia 10% solution, chloroform, ether, magnesium powder, amyl alcohol, vanillin sulfate 10%, hydrochloric acid, potassium hydroxide 5%, ferric chloride, gelatin 1% solution, sodium nitroprusside in alkaline pyridine, sodium hydroxide, and technical-grade 70% ethanol (Brataco Chemika, Bandung, Indonesia).

The chemicals for the determination of total phenolics were gallic acid (Sigma-Aldrich CAS 149-91-7, Sigma-Aldrich Singapore), sodium carbonate (Merck CAS 497-19-8, Merckmillipore Indonesia), ethanol (analytical grade) (Merck Millipore CAS 64-17-5, Merckmillipore Indonesia), and Folin–Ciocâlteu's phenol reagent (F9252 Sigma-Aldrich, Sigma-Aldrich Singapore). The standard for the determination of total flavonoids was quercetin hydrate (Sigma-Aldrich CAS 6151-25-3, Sigma-Aldrich Singapore).

The chemicals for the radical scavenging capacity assay were 1,1-diphenyl-2-picrylhydrazyl (DPPH) free radicals (Tokyo Chemical Industry CAS RN 1898-66-4), L(+)-ascorbic acid (EMSURE Merck CAS 50-81-7), and quercetin hydrate (Sigma-Aldrich CAS 6151-25-3, Sigma-Aldrich Singapore).

2.3. Plant Extraction

Each of the rhizomes of the plants was cleaned from the soil, dust, and other foreign inorganic matter, washed, sliced, and sun-dried. A quantity of 500 g of the dried plant was soaked in ethanol 70% for 24 h at 25 ± 1 °C. Ethanol was selected as the solvent because it is a universal solvent that has the capability to dissolve many secondary metabolites and is a good solvent for flavonol extraction. Furthermore, ethanol is safe for human consumption [19,20].

The extract was filtered using a Whatman paper, and the residue was re-extracted for 2 × 24 h and collected. The solvent was evaporated in a vacuum rotavapor at 45 ± 5 °C, 80 rotations per minute, followed by evaporation in a water bath at 50 ± 1 °C until a thick consistency was obtained. The ethanol extract of *C. heyneana* (25 g) was further partitioned using a mixture of 25 mL of water and 25 mL of *n*-hexane in a separatory funnel. The *n*-hexane phase was collected and was added with 25 mL of ethyl acetate to obtain the ethyl acetate fractions. The same procedure was carried out for *C. zedoaria* (25 g). Ethyl acetate is a semipolar solvent that is widely used to extract polyphenols or flavonols. Partitioning using ethyl acetate was reported to successfully yield the highest amount of total phenolic metabolites [19].

2.4. Phytochemical Screening and Total Phenolics

The thick extract was phytochemically screened by following a previous method [21] as follows:

- Flavonoids were detected by treating the extracts with a few drops of lead acetate solution, which resulted in the formation of a yellow precipitate.
- Phenols were detected by treating the extracts with 3–4 drops of ferric chloride solution, which resulted in the formation of a dark blue color.

- Tannins were detected by treating the extracts with a 1% gelatin solution containing sodium chloride, which resulted in the formation of a white precipitate.
- Alkaloids were detected by treating the extracts with dilute hydrochloric acid and added with the Dragendorff reagent, which resulted in the formation of a red precipitate.
- Glycosides were detected by treating the extracts with sodium nitroprusside in pyridine and sodium hydroxide, which resulted in the formation of a pink to dark red color.
- Saponins were detected by treating the extracts with 20 mL of distilled water and were shaken in a graduated cylinder for 15 min. The formation of a 1 cm layer of foam indicates the presence of saponins.
- Phytosterols were detected by treating the extracts with chloroform and the Liebermann–Burchard reagent, which resulted in the formation of a brown ring at the junction.

The total phenolic compounds were measured as equivalent to gallic acid using the Folin–Ciocâlteu colorimetry method described elsewhere [22,23] with modifications.

2.5. Radical Scavenging Capacity Assay Using the DPPH Method

The antioxidant activity of the plant extracts was evaluated using the DPPH method as described by Ayele and co-workers [23] with modifications. Briefly, an accurately weighed 20 mg of DPPH was dissolved in analytical-grade methanol in a 500 mL volumetric flask to obtain a concentration of 40 µg/mL.

The standards used were ascorbic acid and quercetin. A solution of ascorbic acid was prepared by dissolving 10 mg of ascorbic acid in 250 mL of methanol, and a solution of quercetin was prepared by dissolving 10 mg of quercetin in 250 mL of methanol. The standard addition curves were generated by preparing different concentrations, i.e., 0.41, 1.02, 2.56, 6.4, 16, and 40 µg/mL, of the standard solutions.

To each microplate well, 100 µL of standard and 100 µL of DPPH solutions were added; then, the plate was covered with aluminum foil and kept in the dark for 30 min. For the extracts, 100 µL of 5.12, 12.8, 32.0, 80.0, 200.0, and 500 µg/mL of the extracts were mixed with 100 µL of DPPH in a microplate well. The mixture was kept in the dark for 30 min. Finally, the absorbance was measured at 517 nm.

The % radical scavenging capacity (or % inhibition of DPPH radicals) was calculated using Equation (1) as follows:

$$\text{the percentage (\%) of inhibition} = \frac{A_{DPPH} - A_{sample}}{A_{DPPH}} \times 100\% \quad (1)$$

where A_{DPPH} = the absorbance of DPPH in methanol and A_{sample} = the absorbance of the extract.

The DPPH radical solution had a purple color before the reaction, and after it was reacted with the antioxidant of the extract, the color changed to pale yellow due to the formation of a stable DPPH-H.

IC_{50} values were calculated from the plotted graph of the radical scavenging capacity against the various concentrations of extracts using the GraphPad Prism version 8.0 software to obtain a 4PL (4-parameter logistic) written in Equation (2) as follows:

$$y = d + \frac{a - d}{1 + \left(\frac{x}{c}\right)^b} \quad (2)$$

a = the minimum value that can be obtained (at 0); d = the maximum value that can be obtained; c = the point of inflection; b = Hill's slope of the curve (the steepness of the cure at point c); y = the dependent variable; x = the independent variable (concentration).

IC_{50} (in µg/mL) is defined as the capacity to reduce the initial DPPH radical concentration by 50%.

2.6. Liquid Chromatography–Mass Spectroscopy (LC-MS) for the Total Flavonoid Content Analysis

Quercetin was used as the standard in the total flavonoid content analysis because it is an important bioactive metabolite found in numerous plants. It is categorized in the class of flavonoids and has been reported for its extensive pharmacology activities [24]. Previous studies have described that the commonly used method for the analysis of quercetin is liquid chromatography, e.g., LC-MS [25,26], HPLC [27–30], and UPLC [31,32].

The quercetin standard solution was prepared by dissolving an accurately weighed 10 mg of quercetin (using a Mettler Toledo MS 204TS digital analytical balance) in 100 mL of analytical-grade ethanol. The solution was diluted to obtain a concentration of 10 µg/mL.

The extract solution was prepared by dissolving 100 mg of extract with the highest phenolic content in 100 mL of analytical-grade ethanol to obtain a concentration of 1000 µg/mL. A volume of 15 mL extract 1000 µg/mL was put into five volumetric flasks (25 mL in capacity). A variation volume of quercetin standard solution was put into the flasks to obtain quercetin concentrations of 0, 4, 8, 16, and 32 µg/mL, respectively. The solutions were filtered using Millipore membrane 0.2 µm, and each 5 µL of the solution was injected into the AcquityTM Ultra Performance LC BEH shield RP18 1.7 µm, 2.1 × 100 mm column (part no. 186002352, serial no. 01853023815719) embedded in a Waters AcquityTM Ultra Performance LC instrument. The mobile phase system was a mixture of phase A (water and formic acid) and phase B (methanol). The flow rate was set at 0.2 mL/minute.

The mass spectroscopy system used in tandem with the LC was a Waters XevoTM Qtof MS in positive ESI ionization mode, scanned at the range of 50–1000 *m/z,* with the source temperature at 100 °C, the de-solvated temperature at 350 °C, and a cone N_2 gas flow of 15 L/h. The LC chromatogram and the MS spectra were compared to those of the standard quercetin.

2.7. Molecular Docking Simulation

2.7.1. Hardware

The hardware used was a MacBook Pro (13-inch, M1, 2020), macOS Ventura, with an Apple M1 processor chip and a memory of 8 GB.

2.7.2. Preparation of the Macromolecule

The X-ray crystallographic 3D structure of the tyrosinase enzyme was isolated from *Bacillus megaterium* in complex with the kojic acid inhibitor (PDB ID 3NQ1 with a resolution of 2.3 Å; DOI: https://doi.org/10.2210/pdb3NQ1/pdb, accessed on 10 March 2023) deposited by Sendovski et al. (2011) [33]. The protein was downloaded from the Protein Data Bank (https://www.rcsb.org/ accessed on 10 March 2023). SwissPDBViewer v.4.01 (downloaded from https://spdbv.unil.ch/ accessed on 10 March 2023) was used to separate the chains and fix the macromolecule. Hydrogens were added to the macromolecule PDB, followed by the calculation of their partial charges.

2.7.3. Preparation of the Ligand

The 2D structures of the ligands (ethyl *p*-methoxycinnamate, 6-gingerol, galangin, and kaempferol) and standard ligands (arbutin, kojic acid, and hydroquinone) were built using ChemDraw 12.0 and saved in .cdx format. The geometry optimization of the ligands was performed by applying the molecular mechanic 2 (MM2), and the optimized ligands were saved in .pdb format [34,35].

2.7.4. Molecular Docking Simulation

This step was performed using AutoDock Vina by docking the four phenolic compounds and the three standards as the ligands in the catalytic site of tyrosinase. The binding affinity in terms of the docking score (kcal/mol), the hydrogen bond and the hydrophobic interactions, and the close contact residues were recorded and compared.

3. Results

3.1. Phytochemical Screening, Total Phenolics, and Radical Scavenging Capacity

Phytochemical screening of the plant extracts revealed the presence of flavonoids and polyphenols in the rest of the tested plants. The total phenols and the radical scavenging activity of the plants are summarized in Table 1. The ethanol extract of the *Alpinia galanga* rhizome demonstrated the highest phenolic level (252.36 mg GAE/g extract) and antioxidant activity (IC_{50} of 66.67 µg/mL); therefore, it was further analyzed by the LC-MS method.

Furthermore, the association between total phenolics and radical scavenging activity was analyzed using the Pearson correlation, which resulted in a moderate correlation between the two variables (r = 0.6206) (Figure 2).

Table 1. Total phenolics and radical scavenging capacity of the Zingiberaceae plants.

Tested Plant	Total Phenolics (Equivalent to mg GAE/g Extract) Using Folin–Ciocâlteu (Linear Regression Equation Obtained from the Calibration Graph)	DPPH Radical Scavenging Capacity Presented as an IC_{50} Value in µg/mL
H. coronarium rhizome (ethanol extract)	31.03 ($y = 0.0114x + 1.4152$, $R^2 = 0.9933$)	243.40 (weak)
C. zedoaria rhizome (ethanol extract)	17.92 ($y = 0.0556x + 0.1594$, $R^2 = 0.9773$)	251.70 (weak)
C. zedoaria rhizome (ethyl acetate fraction)	22.54 ($y = 0.0343x + 0.1237$, $R^2 = 0.9936$)	171.86 (weak)
C. heyneana rhizome (ethanol extract)	83.69 ($y = 0.0668x + 0.1789$, $R^2 = 0.9945$)	320.00 (weak)
C. heyneana rhizome (ethyl acetate fraction)	90.32 ($y = 0.0388x + 0.1897$, $R^2 = 0.9847$)	298.80 (weak)
A. galanga rhizome (ethanol extract)	252.36 ($y = 2.5013x + 3.4161$, $R^2 = 0.9901$)	66.67 (moderate)
Ascorbic acid		1.39 (strong)
Quercetin		0.59 (strong)

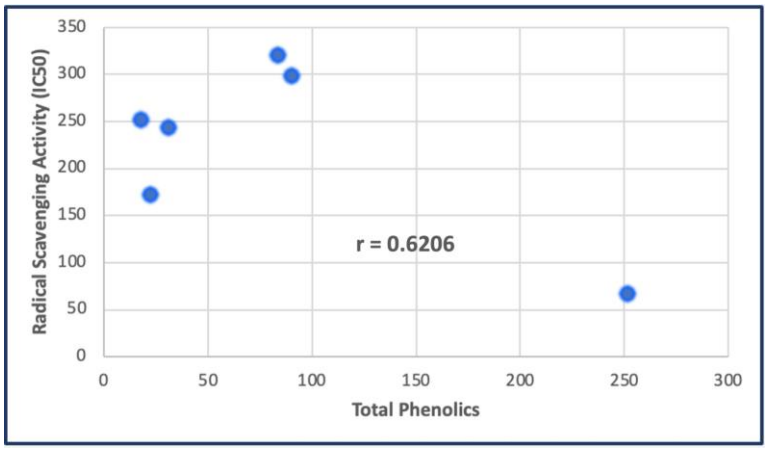

Figure 2. Pearson correlation analysis graph of the association between total phenolics and radical scavenging activity, resulting in a correlation coefficient of r = 0.6206. The blue dots indicate the data of the two variables (IC_{50} value and total phenolics).

3.2. LC-MS Analysis of A. galanga Extract

The LC chromatogram of *A. galanga* is depicted in Figure 3a and the MS spectrum of *A. galanga* is shown in Figure 3b. The total flavonoids calculated as quercetin in the extract were determined using a standard addition method, and the resulting curve, which is a plot between the area under the curve (AUC) and the concentration of standard quercetin, is presented in Figure 4.

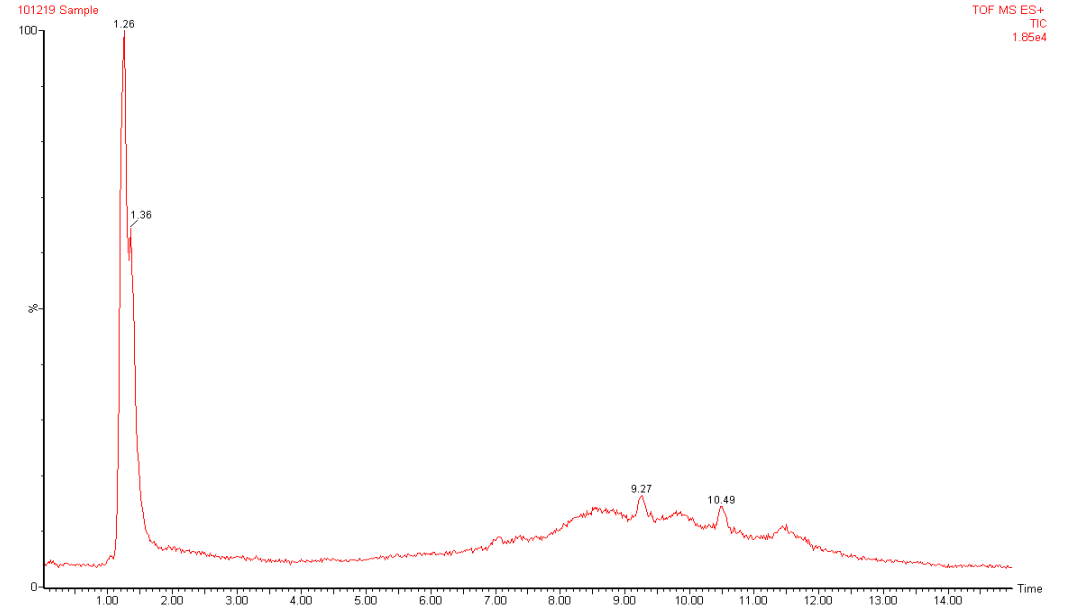

(**a**)

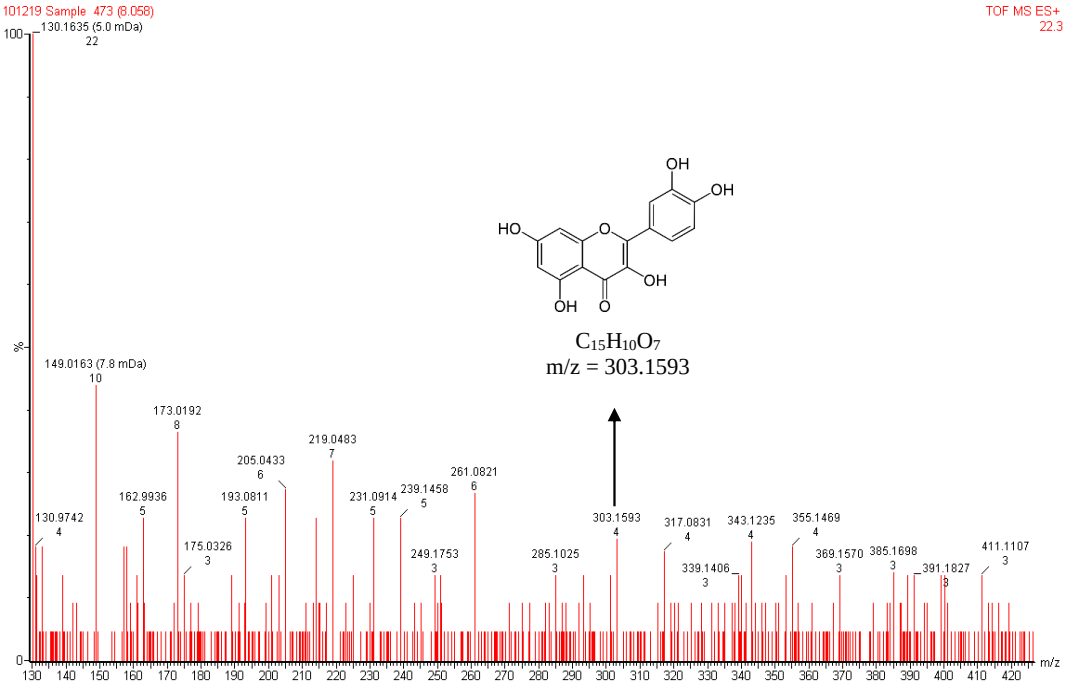

(**b**)

Figure 3. (**a**) LC chromatogram and (**b**) MS spectrum of *A. galanga* rhizome extract. Quercetin was confirmed to be present in the *A. galanga* extract, as shown by a small peak at 9.27 min (similar to standard quercetin eluted at 9.16 min) and an MS peak at *m*/*z* 303.1593.

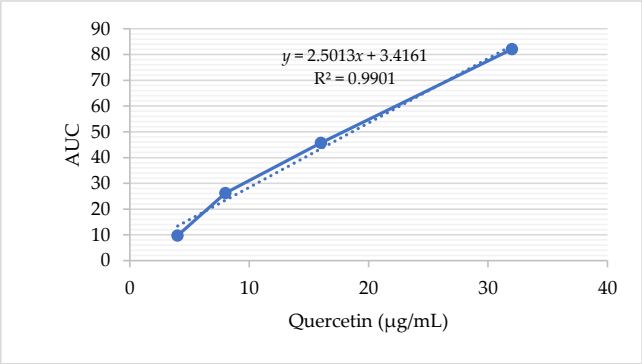

Figure 4. The standard addition curve of quercetin spiked to the *Alpinia galanga* rhizome extract resulted in a linear regression equation of $y = 2.5013x + 3.4161$, with a coefficient of correlation R^2 of 0.9901.

By using the standard addition curve, the amount of quercetin in *A. galanga* extract was calculated and resulted in 0.378% *w/w*.

3.3. Molecular Docking Simulation

A molecular docking simulation revealed that known constituents of *A. galanga* could occupy the catalytic site of tyrosinase and interact with essential residues. Although kaempferol showed the strongest binding affinity towards tyrosinase, as proven by its smallest docking score of −7.6 kcal/mol, galangin is considered the best ligand based on its similar binding mode to that of kojic acid. Galangin also demonstrated a strong binding affinity which is comparable with that of kaempferol. The results are summarized in Table 2.

Table 2. Molecular docking simulation of kaempferol, galangin, ethyl *p*-methoxy cinnamate, and 6-gingerol with residues in the catalytic site of tyrosinase. Arbutin, kojic acid, and hydroquinone were employed as the standards.

Phenol Compound (Ligand)	Binding Affinity in Terms of Docking Score (kcal/mol)	Residues Involved in the Hydrogen Bond Interaction (Distance in Å)	Residues Involved in the Hydrophobic Interaction (Distance in Å)	Close Contact Residues in the Catalytic Site
Kaempferol	−7.6	N/A	Pro201 (3.6–3.7 Å)	Glu158, Gly200, Pro201, His208, Arg209, Gly216, Val 218, Cu501, Cu502
Galangin	−7.1	Gly216 (1.754 Å)	Asn205 (3.6 Å) His208 (3.9 Å) Gly216 (3.9 Å) Val218 (3.6–3.7 Å)	Asn205, His208, Gly216, Val218, Cu501
Arbutin	−6.5	Asn205 (2.075 Å)	Pro201 (3.5–3.8 Å) Arg209 (3.6–3.9 Å)	Pro201, His204, Asn205, Arg209, Val218
Ethyl *p*-methoxy cinnamate	−5.7	N/A	Pro201 (3.6–3.9 Å) Asn205 (3.6–3.9 Å) Arg209 (3.7–3.9 Å)	Met184, Pro201, Asn205, Arg209
Kojic Acid	−5.6	N/A	His204 (3.7 Å) His208 (3.6–3.9 Å) Gly216 (3.8 Å)	His204, His208, Cu501, Cu502
6-Gingerol	−5.4	N/A	Asn205 (3.6 Å) Arg209 (3.5–3.9 Å) Gly216 (3.7 Å) Val218 (3.6–3.7 Å)	His60, Asn205, His208, Arg209, Gly216, Val218, Cu501
Hydroquinone	−5.4	Met215 (1.885 Å)	N/A	His60, Asn205, His208, Met215, Val217, Val218, Cu501

The 2D and 3D structure of galangin, the total charge density and the electrostatic potential map, and the molecular interaction of galangin with tyrosinase are presented in Figure 5. Galangin interacts with tyrosinase by building one hydrogen bond to Gly216 at a distance of 1.754 Åand hydrophobic interactions with Asn205, His208, Gly216, and Val218. Hydrophobic interaction with His208 and Gly216 was also shown by kojic acid.

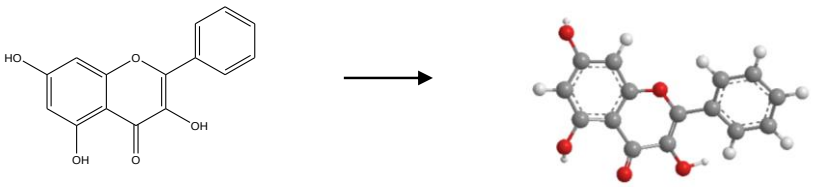

(**a**)

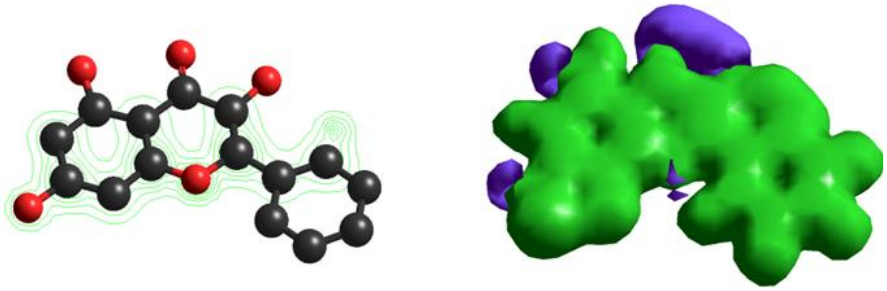

(**b**)

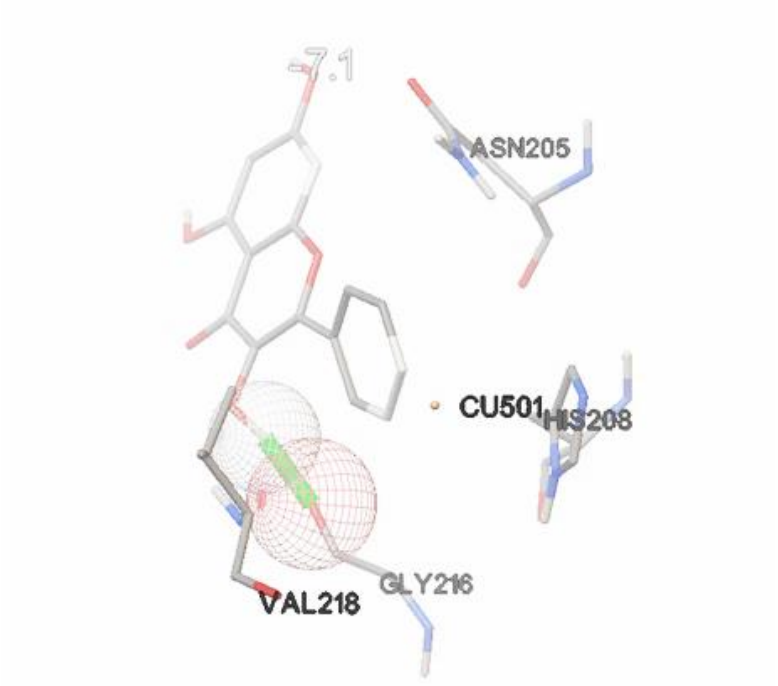

(**c**)

Figure 5. Galangin with a molecular weight of 270.24, cLog P of 2.37, and volume of 718.24 Å^3: (**a**) the 2D and 3D structure; (**b**) the total charge density (**left**) and the electrostatic potential map (**right**). The green color indicates the electropositive region, the violet color is the electronegative; and (**c**) the molecular interaction with tyrosinase residues in the catalytic site of the enzyme. The copper ion is labeled as CU501. The pink spheres indicate the hydrogen bond.

4. Discussion

Phenolics, e.g., flavonols, are plants' multifunctional metabolites that react with free radicals through several mechanisms, such as (a) reductors, (b) radical scavengers, (c) metal chelators, and (d) singlet oxygen quenchers [36]. Phenolics have been confirmed for their antioxidant activity [37,38]. Moreover, a positive correlation between phenolic contents and antioxidant activity was previously confirmed [39].

Similarly, our study reveals that the levels of phenolics in Zingiberaceae plants are highly varied, with the highest contents being found in the *Alpinia galanga* rhizome (252.36 mg GAE/g extract), the *C. heyneana* rhizome (83.69 mg GAE/g extract), the *H. coronarium* rhizome (31.03 mg GAE/g extract), and the *C. zedoaria* rhizome (17.92 mg GAE/g extract). The phenolic levels are in a moderate correlation (r = 0.6206) with the radical scavenging capacity of the plant extracts, confirming that phenolics are indicators of antioxidant properties.

Comparable to our results, a previous study reported that the total phenolics of *C. zedoaria* collected in Kanchanaburi, Thailand, in 2013 was 9.3 $\pm$ 0.7 mg GAE/g extract [40]. Another study conducted in Saudi Arabia described that the phenolic contents of *A. galanga*, obtained from the local market in Riyadh, were 53.18 mg GAE/g extract [41], indicating a smaller amount compared to the present study.

The plant with the highest phenolic levels further had its quercetin levels determined (total flavonoids calculated as quercetin) using the liquid chromatography in tandem with mass spectrometry (LC-MS) method, which resulted in the evidence that quercetin is present in *A. galanga* extract, as proven by a small peak at 9.27 min (similar to standard quercetin eluted at 9.16 min) and confirmed by an MS peak at m/z 303.1593 (the molecular weight of quercetin), in an amount of 0.378% *w/w*.

Our result is in accordance with, although lower than, that given in a previous work of Suzery et al. (2019), who reported that quercetin in the ethyl acetate fraction of *A. galanga* collected from Banyumanik, Central Java, Indonesia, was 0.5469% *w/w* [42]. Discovering plants with high levels of phenolics and strong antioxidant properties is beneficial for the development of novel drugs and cosmetics.

When free oxygen radicals are formed in the body, the enzyme superoxide dismutase (SOD) immediately catches the oxygen anions (O^{2-}) and converts them to peroxides (H_2O_2). The enzyme then catalyzes the degradation of H_2O_2 to nontoxic water molecules (H_2O) with the help of glutathiones (GSH). It was announced that quercetin, a flavonol, could stimulate the production of GSH in animal models [43–45]. Quercetin has been widely reported to possess the capacity to give its hydrogen atoms and to extinguish the reactivity of oxygen radicals due to its phenolic hydroxyl group and double bond [46]. In vitro studies confirmed that quercetin significantly reduced the levels of inflammatory mediators, e.g., NO synthase, COX-2, and C-reactive protein, in human hepatocyte-derived cell lines [47]. A combination of quercetin with glutathione was described to show a synergy. The observed synergy was parallel with the glutathione content, elevating up to the 1:16 ratio and then decreasing [48]. Studies in humans reported that quercetin significantly decreased plasma concentrations of atherogenic oxidized low-density lipoproteins but did not significantly alter TNF-α and C-reactive protein when compared with placebo [49]. A randomized clinical trial to determine the safety of quercetin therapy in patients with chronic obstructive pulmonary disease confirmed that this flavonol is safely tolerated up to a dose of 2000 mg per day [50]. Interestingly, a recently published article reported that quercetin treatment in patients with early-stage COVID-19 resulted in speedy clearance of SARS-CoV-2, faster recovery of the acute symptoms, and modulation of the host's hyperinflammatory response [51]. However, despite the advantages of quercetin in ameliorating COVID-19 infection and symptoms, it was thought that further clinical trials are needed to strongly establish its clinical efficacy against COVID-19 [52].

Our molecular docking simulation revealed that the phytoconstituents of *A. galanga* could settle in the catalytic site of tyrosinase by interacting with essential residues. Although kaempferol showed the strongest binding affinity towards tyrosinase, as proven by its

smallest docking score of −7.6 kcal/mol, galangin (docking score of −7.1 kcal/mol) is considered the best ligand based on its similar binding mode to that of kojic acid. Galangin also demonstrated a strong binding affinity, which is comparable with that of kaempferol.

Numerous flavonols have been reported for their activity in inhibiting tyrosinase by competitively blocking the oxidation of the substrate L-DOPA (dihydroxyphenylalanine) into dopachrome and melanin by tyrosinase. This inhibitory activity is performed by chelating the copper in the enzyme's catalytic site. The order of the flavonols with respect to their inhibitory activity toward tyrosinase, from the highest to the lowest, is quercetin > myricetin > kaempferol > galangin. However, compared to kojic acid, the inhibitory activity of these flavonols is weaker [53]. Kojic acid, a strong whitening ingredient in cosmetics, is a slow-binding inhibitor of tyrosinase in its active form [54]. Kojic acid, co-crystallized in tyrosinase by Sendovski and co-workers [33], binds to the catalytic site of the enzyme by building hydrophobic interactions with Asn205 and Gly196 (Figure 6).

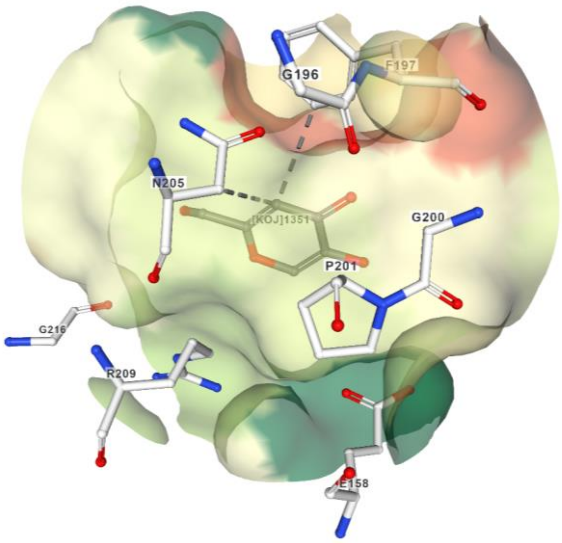

Figure 6. Kojic acid binds to the catalytic site of tyrosinase (downloaded from https://www.rcsb.org/structure/3NQ1 (accessed on 10 August 2023) PDB DOI: https://doi.org/10.2210/pdb3NQ1/pdb, accessed on 10 August 2023; Deposition Author(s): Sendovski, M.; Kanteev, M.; Adir, N.; Fishman, A.; and viewed using NGL (WebGL)). The different colors demonstrate the opacity (the lack of transparency) of the binding pocket based on the hydrophobicity [33].

Tyrosinase is a metalloenzyme containing copper ions in its catalytic site, which functions as a rate-limiting enzyme in melanin biosynthesis. The catalytic role of this enzyme comprises (1) the monophenolase activity, where it hydroxylates the monophenols to *orto*-diphenols, and (2) the diphenolase activity, where tyrosinase oxidizes *orto*-diphenols to *orto*-quinones [55]. According to our molecular docking simulation, kojic acid does not interact with Asn205, though hydrophobic interactions with His204 (3.7 Å), His208 (3.6–3.9 Å), and Gly216 (3.8 Å) were observed. Interestingly, our tested phenolic compound, namely, galangin, also builds hydrophobic interactions with Asn205 (3.6 Å), His208 (3.9 Å), Gly216 (3.9 Å), and Val218 (3.6–3.7 Å) and one hydrogen bond with Gly216 (1.754 Å), as shown in Figure 5 and summarized in Table 2.

5. Conclusions

The present study confirms that phenolic compounds and/or flavonols are the main contributors to the radical scavenging capacity of Zingiberaceae plants. The limitation of this study is that the number of plants assayed may not represent the whole plant family, thus opening the chance for the researchers to further investigate medicinal plants belonging to the Zingiberaceae family. It should be noted that, of the four assayed plants, the ethanol extract of the *Alpinia galanga* rhizome demonstrated the highest phenolic

level (252.36 mg GAE/g extract) and a moderate radical scavenging activity (IC_{50} of 66.67 μg/mL). Quercetin is present in this plant extract in a low amount. Moreover, the phytoconstituents of *A. galanga*, e.g., kaempferol, galangin, ethyl *p*-methoxycinnamate, and 6-gingerol, could occupy the binding site of tyrosinase with prominent affinity and interact with essential residues of the enzyme, and of these, galangin shows the best binding mode, similar to that of kojic acid. These findings may suggest the potential of *A. galanga* extract as an active component in cosmetics, particularly skin-whitening products.

Author Contributions: Conceptualization, M. and J.L.; methodology, M.; software, S.M.; validation, M., F.A.S. and R.A.; formal analysis, R.A. and N.M.S.; investigation, J.L.; resources, M. and S.A.S.; data curation, M. and J.L.; writing—original draft preparation, M. and J.L.; writing—review and editing, F.A.S. and J.L.; project administration, M. and S.A.S.; funding acquisition, M. All authors have read and agreed to the published version of the manuscript.

Funding: This research was funded by Padjadjaran University via the Directorate of Research and Community Engagement in the scheme of the Academic Leadership Grant years 2020-2023 of Prof. Jutti Levita, and the APC was funded by Padjadjaran University.

Institutional Review Board Statement: Not applicable.

Informed Consent Statement: Not applicable.

Data Availability Statement: No new data were created or analyzed in this study. Data sharing is not applicable to this article.

Conflicts of Interest: The authors declare no conflict of interest.

References

1. Salmerón-Manzano, E.; Garrido-Cardenas, J.A.; Manzano-Agugliaro, F. Worldwide research trends on medicinal plants. *Int. J. Environ. Res. Public Health* **2020**, *17*, 3376. [CrossRef]
2. Trugo, L.; Finglas, P.M. (Eds.) *Encyclopedia of Food Sciences and Nutrition*, 2nd ed.; Academic Press: Cambridge, MA, USA, 2003.
3. Spiegel, M.; Andruniów, T.; Sroka, Z. Flavones' and flavonols' antiradical structure-activity relationship—A quantum chemical study. *Antioxidants* **2020**, *9*, 461. [CrossRef]
4. Yao, L.H.; Jiang, Y.M.; Shi, J.; Tomás-Barberán, F.A.; Datta, N.; Singanusong, R.; Chen, S.S. Flavonoids in food and their health benefits. *Plant Foods Hum. Nutr.* **2004**, *59*, 113–122. [CrossRef]
5. Masek, A.; Chrzescijanska, E.; Latos, M.; Zaborski, M. Influence of hydroxyl substitution on flavanone antioxidants properties. *Food Chem.* **2017**, *215*, 501–507. [CrossRef] [PubMed]
6. Amić, A.; Marković, Z.; Klein, E.; Dimitrić Marković, J.M.; Milenković, D. Theoretical study of the thermodynamics of the mechanisms underlying antiradical activity of cinnamic acid derivatives. *Food Chem.* **2018**, *246*, 481–489. [CrossRef] [PubMed]
7. Ramli, M.R.; Milow, P.; Malek, S. Diversity and traditional knowledge of medicinal plants in home gardens of Kampung Masjid Ijok, Perak, Malaysia. *Biodiversitas* **2021**, *22*, 2458–2465. [CrossRef]
8. Kubo, I.; Kinst-Hori, I.; Chaudhuri, S.K.; Kubo, Y.; Sánchez, Y.; Ogura, T. Flavonols from *Heterotheca inuloides*: Tyrosinase inhibitory activity and structural criteria. *Bioorg. Med. Chem.* **2000**, *8*, 1749–1755. [CrossRef] [PubMed]
9. Matsuda, H.; Nakashima, S.; Oda, Y.; Nakamura, S.; Yoshikawa, M. Melanogenesis inhibitors from the rhizomes of *Alpinia officinarum* in B16 melanoma cells. *Bioorg. Med. Chem.* **2009**, *15*, 6048–6053. [CrossRef]
10. Huang, H.C.; Chang, S.J.; Wu, C.Y.; Ke, H.J.; Chang, T.M. [6]-Shogaol inhibits α-MSH-induced melanogenesis through the acceleration of ERK and PI3K/Akt-mediated MITF degradation. *BioMed Res. Int.* **2014**, *2014*, 842569. [CrossRef]
11. Chigurupati, S.; Al-Murikhy, A.; Almahmoud, S.A.; Almoshari, Y.; Saber Ahmed, A.; Vijayabalan, S.; Ghazi Felemban, S.; Raj Palanimuthu, V. Molecular docking of phenolic compounds and screening of antioxidant and antidiabetic potential of Moringa oleifera ethanolic leaves extract from Qassim region, Saudi Arabia. *Saudi J. Biol. Sci.* **2022**, *29*, 854–859. [CrossRef]
12. Lekmine, S.; Benslama, O.; Kadi, K.; Martín-García, A.I.; Yilmaz, M.A.; Akkal, S.; Boumegoura, A.; Alhomida, A.S.; Ola, M.S.; Ali, A. LC/MS-MS analysis of phenolic compounds in Hyoscyamus albus L. extract: In vitro antidiabetic activity, in silico molecular docking, and in vivo investigation against STZ-induced diabetic mice. *Pharmaceuticals* **2023**, *16*, 1015. [CrossRef] [PubMed]
13. Kurnia, D.; Putri, S.A.; Tumilaar, S.G.; Zainuddin, A.; Dharsono, H.D.A.; Amin, M.F. In silico study of antiviral activity of polyphenol compounds from *Ocimum basilicum* by molecular docking, ADMET, and drug-likeness analysis. *Adv. Appl. Bioinform. Chem.* **2023**, *16*, 37–47. [CrossRef] [PubMed]
14. Baruah, I.; Kashyap, C.; Guha, A.K.; Borgohain, G. Insights into the interaction between polyphenols and β-lactoglobulin through molecular docking, MD simulation, and QM/MM approach. *CS Omega* **2022**, *7*, 23083–23095.
15. Lešnik, S.; Bren, U. Mechanistic insights into biological activities of polyphenolic compounds from rosemary obtained by inverse molecular docking. *Foods* **2022**, *11*, 67. [CrossRef]

16. Lescano, C.H.; de Lima, F.F.; Mendes-Silvério, C.B.; Justo, A.F.O.; da Silva Baldivia, D.; Vieira, C.P.; Sanjinez-Argandoña, E.J.; Cardoso, C.A.L.; Mónica, F.Z.; de Oliveira, I.P. Effect of polyphenols from *Campomanesia adamantium* on platelet aggregation and inhibition of cyclooxygenases: Molecular docking and in vitro analysis. *Front. Pharmacol.* **2018**, *9*, 617. [CrossRef]
17. Raal, A.; Meos, A.; Hinrikus, T.; Heinämäki, J.; Romāne, E.; Gudienė, V.; Jak Tas, V.; Koshovyi, O.; Kovaleva, A.; Fursenco, C.; et al. Dragendorff's reagent: Historical perspectives and current status of a versatile reagent introduced over 150 years ago at the University of Dorpat, Tartu, Estonia. *Die Pharm.* **2020**, *75*, 299–306.
18. Adu, J.K.; Amengor, C.D.K.; Kabiri, N.; Orman, E.; Patamia, S.A.G.; Okra, B.K. Validation of a simple and robust Liebermann–Burchard colorimetric method for the assay of cholesterol in selected milk products in Ghana. *Int. J. Food Sci.* **2019**, *2019*, 9045938. [CrossRef]
19. Dai, J.; Mumper, R.J. Plant phenolics: Extraction, analysis and their antioxidant and anticancer properties. *Molecules* **2010**, *15*, 7313–7352. [CrossRef]
20. Scarano, P.; Tartaglia, M.; Zuzolo, D.; Prigioniero, A.; Guarino, C.; Sciarrillo, R. Recovery and valorization of bioactive and functional compounds from the discarded of *Opuntia ficus-indica* (L.) Mill. fruit peel. *Agronomy* **2022**, *12*, 388. [CrossRef]
21. Tiwari, P.; Kumar, B.; Kaur, M.; Kaur, G.; Kaur, H. Phytochemical screening and extraction: A review. *Int. Pharm. Sci.* **2011**, *1*, 98–106.
22. Nakamura, M.; Ra, J.-H.; Jee, Y.; Kim, J.-S. Impact of different partitioned solvents on chemical composition and bioavailability of *Sasa quelpaertensis* Nakai leaf extract. *J. Food Drug Anal.* **2017**, *25*, 316–326. [CrossRef]
23. Ayele, D.T.; Akele, M.L.; Melese, A.T. Analysis of total phenolic contents, flavonoids, antioxidant and antibacterial activities of *Croton macrostachyus* root extracts. *BMC Chem.* **2022**, *16*, 30. [CrossRef]
24. Yang, D.; Wang, T.; Long, M.; Li, P. Quercetin: Its main pharmacological activity and potential application in clinical medicine. *Oxid. Med. Cell. Longev.* **2020**, *2020*, 8825387. [CrossRef] [PubMed]
25. Panchal, H.; Shah, M.B. Development and validation of a rapid LC-MS/MS method for simultaneous determination of kaempferol and quercetin in *Thespesia populnea* Extract. *J. AOAC Int.* **2017**, *100*, 971–975. [CrossRef] [PubMed]
26. Ni, B.; Cao, S.; Feng, L.; Yin, X.; Wang, W.; Zhang, X.; Ni, J. Simultaneous analysis of quercetin and naringenin in rat plasma by liquid chromatography–tandem mass spectrometry: Application to a pharmacokinetic study after oral administration. *J. Chromatogr. Sci.* **2016**, *54*, 1359–1364. [CrossRef] [PubMed]
27. Pandey, J.; Bastola, T.; Tripathi, J.; Tripathi, M.; Rokaya, R.K.; Dhakal, B.; Rabin, D.C.; Bhandari, R.; Poudel, A. Estimation of total quercetin and rutin content in *Malus domestica* of Nepalese origin by HPLC method and determination of their antioxidative activity. *J. Food Qual.* **2020**, *2020*, 8853426. [CrossRef]
28. Park, J.S.; Kim, I.S.; Ur Rehman, S.; Na, C.-S.; Yoo, H.H. HPLC Determination of bioactive flavonoids in *Hovenia dulcis* fruit extracts. *J. Chromatogr. Sci.* **2016**, *54*, 130–135.
29. Ang, L.F.; Yam, M.F.; Fung, Y.T.; Kiang, P.K.; Darwin, Y. HPLC method for simultaneous quantitative detection of quercetin and curcuminoids in traditional Chinese medicines. *J. Pharmacopunct.* **2014**, *17*, 36–49. [CrossRef] [PubMed]
30. Lee, J.S.; Paje, L.A.; Choi, W.H.; Cho, E.J.; Kim, H.Y.; Jacinto, S.D.; Lee, S. Validation of an optimized HPLC/UV method for the quantification of flavonoids in lotus. *Appl. Biol. Chem.* **2020**, *63*, 84. [CrossRef]
31. Yao, X.; Zhou, G.; Tang, Y.; Li, Z.; Su, S.; Qian, D.; Duan, J.A. A UPLC-MS/MS method for qualification of quercetin-3-O-β-D-glucopyranoside-(4→1)-α-L-rhamnoside in rat plasma and application to pharmacokinetic studies. *Molecules* **2013**, *18*, 3050–3059. [CrossRef]
32. Gbylik-Sikorska, M.; Gajda, A.; Burmańczuk, A.; Grabowski, T.; Posyniak, A. Development of a UHPLC-MS/MS method for the determination of quercetin in milk and its application to a pharmacokinetic study. *J. Vet. Res.* **2019**, *63*, 87–91. [CrossRef] [PubMed]
33. Sendovski, M.; Kanteev, M.; Ben-Yosef, V.S.; Adir, N.; Fishman, A. First structures of an active bacterial tyrosinase reveal copper plasticity. *J. Mol. Biol.* **2011**, *405*, 227–237. [CrossRef] [PubMed]
34. Firmansyah, D.; Sumiwi, S.A.; Saptarini, N.M.; Levita, J. Molecular interaction of curcumin, demethoxycurcumin, bisdemethoxycurcumin, and turmerone of *Curcuma longa* with tyrosinase and tyrosinase-related protein-1. *Rasayan J. Chem.* **2021**, *14*, 2298–2303. [CrossRef]
35. Megantara, S.; Wathoni, N.; Mohammed, A.F.A.; Suhandi, C.; Ishmatullah, M.H.; Putri, M.F.F.D. In silico study: Combination of α-mangostin and chitosan conjugated with trastuzumab against human epidermal growth factor receptor 2. *Polymers* **2022**, *14*, 2747. [CrossRef] [PubMed]
36. Akhlaghi, M.; Bandy, B. Mechanisms of flavonoid protection against myocardial ischemia-reperfusion injury. *J. Mol. Cell. Cardiol.* **2009**, *46*, 309–317. [CrossRef]
37. Sulaiman, C.T.; Balachandran, I. Total phenolics and total flavonoids in selected Indian medicinal plants. *Indian. J. Pharm. Sci.* **2012**, *74*, 258–260. [CrossRef]
38. Oki, T.; Masuda, M.; Furuta, S.; Nishibia, Y.; Terahara, N.; Suda, I. Involvement of anthocyanins and other phenolic compounds in the radical-scavenging activity of purple-fleshed sweet potato cultivars. *Food Chem. Toxicol.* **2002**, *67*, 1752–1756. [CrossRef]
39. Nampoothiri, S.V.; Esakkidurai, T.; Pitchumani, K. Identification and quantification of phenolic compounds in *Alpinia galanga* and *Alpinia calcarata* and its relation to free radical quenching properties: A comparative study. *J. Herbs Spices Med. Plants* **2015**, *21*, 140–147. [CrossRef]

40. Burapan, S.; Kim, M.; Paisooksantivatana, Y.; Eser, B.E.; Han, J. Thai curcuma species: Antioxidant and bioactive compounds. *Foods* **2020**, *9*, 1219. [CrossRef]
41. Aljobair, M.O. Chemical composition, antimicrobial properties, and antioxidant activity of galangal rhizome. *Food Sci. Technol.* **2022**, *42*, e45622. [CrossRef]
42. Suzery, M.; Ningrum, A.N.; Nudin, B.; Mulyani, N.S.; Cahyono, B. Determination of quercetin and rutin in red galangal rhizomes (*Alpinia purpurata*) and white galangal (*Alpinia galanga*) with high-performance liquid chromatography method. *IOP Conf. Ser. Earth Environ. Sci.* **2019**, *292*, 12–64. [CrossRef]
43. Kobori, M.; Takahashi, Y.; Akimoto, Y.; Sakurai, M.; Matsunaga, I.; Nishimuro, H.; Ippoushi, K.; Oike, H.; Ohnishi-Kameyama, M. Chronic high intake of quercetin reduces oxidative stress and induces expression of the antioxidant enzymes in the liver and visceral adipose tissues in mice. *J. Funct. Foods* **2015**, *15*, 551–560. [CrossRef]
44. Granado-Serrano, A.B.; Martín, M.A.; Bravo, L.; Goya, L.; Ramos, S. Quercetin modulates Nrf2 and glutathione-related defenses in HepG2 cells: Involvement of p38. *Chem. Biol. Interact.* **2012**, *195*, 154–164. [CrossRef] [PubMed]
45. Gessner, D.K.; Ringseis, R.; Eder, K. Potential of plant polyphenols to combat oxidative stress and inflammatory processes in farm animals. *J. Anim. Physiol. Anim. Nutr.* **2017**, *101*, 605–628. [CrossRef]
46. Deepika; Maurya, P.K. Health benefits of quercetin in age-related diseases. *Molecules* **2022**, *27*, 2498. [CrossRef] [PubMed]
47. García-Mediavilla, V.; Crespo, I.; Collado, P.S.; Esteller, A.; Sánchez-Campos, S.; Tuñón, M.J.; González-Gallego, J. The anti-inflammatory flavones quercetin and kaempferol cause inhibition of inducible nitric oxide synthase, cyclooxygenase-2 and reactive C-protein, and down-regulation of the nuclear factor kappaB pathway in Chang Liver cells. *Eur. J. Pharmacol.* **2007**, *557*, 221–229. [CrossRef]
48. Ilyasov, I.; Beloborodov, V.; Antonov, D.; Dubrovskaya, A.; Terekhov, R.; Zhevlakova, A.; Saydasheva, A.; Evteev, V.; Selivanova, I. Flavonoids with glutathione antioxidant synergy: Influence of free radicals inflow. *Antioxidants* **2020**, *9*, 695. [CrossRef]
49. Egert, S.; Bosy-Westphal, A.; Seiberl, J.; Kürbitz, C.; Settler, U.; Plachta-Danielzik, S.; Wagner, A.E.; Frank, J.; Schrezenmeir, J.; Rimbach, G.; et al. Quercetin reduces systolic blood pressure and plasma oxidised low-density lipoprotein concentrations in overweight subjects with a high-cardiovascular disease risk phenotype: A double-blinded, placebo-controlled cross-over study. *Br. J. Nutr.* **2009**, *102*, 1065–1074. [CrossRef]
50. Han, M.K.; Barreto, T.A.; Martinez, F.J.; Comstock, A.T.; Sajjan, U.S. Randomised clinical trial to determine the safety of quercetin supplementation in patients with chronic obstructive pulmonary disease. *BMJ Open Respir. Res.* **2020**, *7*, e000392. [CrossRef]
51. Di Pierro, F.; Khan, A.; Iqtadar, S.; Mumtaz, S.U.; Chaudhry, M.N.A.; Bertuccioli, A.; Derosa, G.; Maffioli, P.; Togni, S.; Riva, A.; et al. Quercetin as a possible complementary agent for early-stage COVID-19: Concluding results of a randomized clinical trial. *Front. Pharmacol.* **2022**, *13*, 1096853. [CrossRef]
52. Pawar, A.; Russo, M.; Rani, I.; Goswami, K.; Russo, G.L.; Pal, A. A critical evaluation of risk to reward ratio of quercetin supplementation for COVID-19 and associated comorbid conditions. *Phytother. Res.* **2022**, *36*, 2394–2415. [CrossRef] [PubMed]
53. Chang, T.S. An updated review of tyrosinase inhibitors. *Int. J. Mol. Sci.* **2009**, *10*, 2440–2475. [CrossRef] [PubMed]
54. Cabanes, J.; Chazarra, S.; Garcia-Carmona, F. Kojic acid, a cosmetic skin whitening agent, is a slow-binding inhibitor of catecholase activity of tyrosinase. *J. Pharm. Pharmacol.* **1994**, *46*, 982–985. [CrossRef] [PubMed]
55. Zolghadri, S.; Bahrami, A.; Hassan Khan, M.T.; Munoz-Munoz, J.; Garcia-Molina, F.; Garcia-Canovas, F.; Saboury, A.A. A comprehensive review on tyrosinase inhibitors. *J. Enzym. Inhib. Med. Chem.* **2019**, *34*, 279–309. [CrossRef]